

MARIUSZ WOSZCZYŃSKI
JAROSŁAW TOKARCZYK
KRZYSZTOF MAZUREK
ANDRZEJ PYTLIK

Monitoring of loads in arch support with wire strain gauge

A concept of measuring the load and geometry of a roadway support with the use of vibrating wire strain gauges and draw-wire sensors is presented. Laboratory and in-situ tests of complete frames of arch supports under load were carried out within the INESI project. The deformations recorded by the vibrating wire strain gauges are similar to those recorded by the strain gauges. FEM strength calculations (which were similar to the results from the stand tests) were also presented.

Key words: transducers with vibrating wire strain gauge, strain measurements, geometry of arch support, testing, FEM analysis

1. INTRODUCTION

Increasing the speed and improving the safety of underground auxiliary mine transportation systems are the main objectives of INESI project (Increased efficiency and safety improvement in underground mining transportation routes) coordinated by the KOMAG Institute of Mining Technology and realized within the Research Fund for Coal and Steel (RFCs). Increasing suspended monorail speeds requires the monitoring of transportation routes. For this purpose, a measuring system that collects information about the loads of a roadway support and the changes in its geometry was suggested.

The structure of the measuring system is presented in Figure 1. All of the electronic components will be designed as intrinsically safe as possible to enable their operation in areas threatened by methane and/or coal dust explosion hazards. It is assumed that the monitoring system consists of measuring modules and data-collecting modules that are connected in series in groups whose numbers will be associated with limits in the power supply. The collected information will be transferred to the next modules and will be read out by an external computer system in the end.

The recording of measuring data and its analysis as well as the generation of warning signals about the hazards associated with deformation of a monorail route are based on the developed expert system (i.e., the software) that can draw conclusions and make decisions acting as human reasoning by using detailed knowledge is the main task of the software cooperating with the hardware module.

Within the initial research work, changes in the design of the side wall arches of the support were suggested for installing the measuring system between the cut elements near the floor. This would require us to cut out a section of a few centimeters from the side wall arch to install the strain gauge. Besides the force transducer, a wire displacement sensor and electronic measuring system will be installed. Measuring the wires of the draw-wire displacement sensor will be led in such a way as to minimize collisions with other roadway components. Here are the functions of the measuring system:

- strain gauge force measurements,
- displacement measurements,
- measurements analyses,
- displaying warning and alarm signals,
- sending information to collecting module.

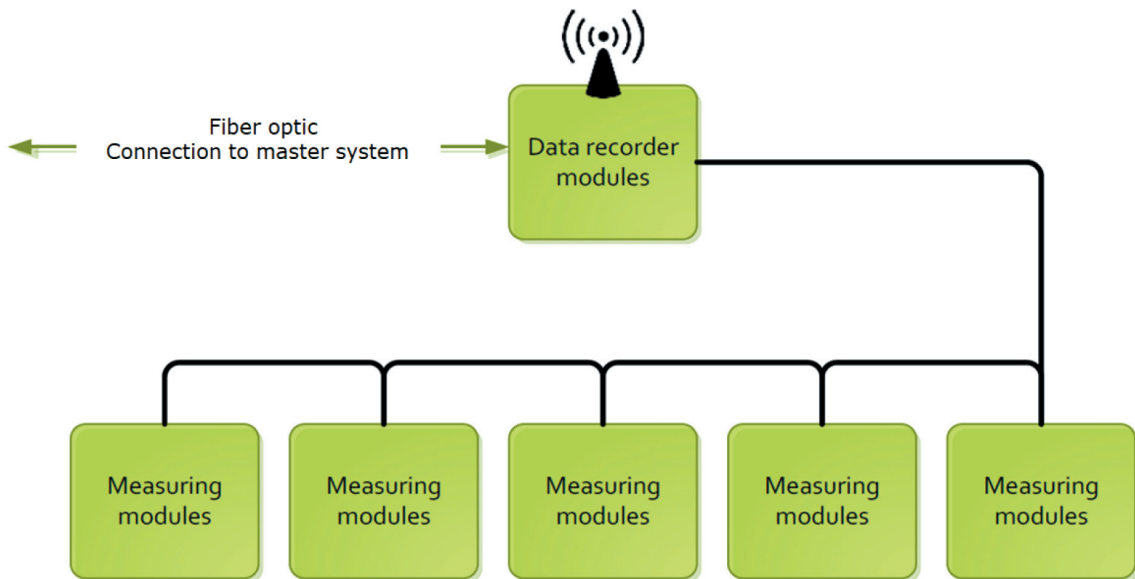


Fig. 1. Structure of measuring system

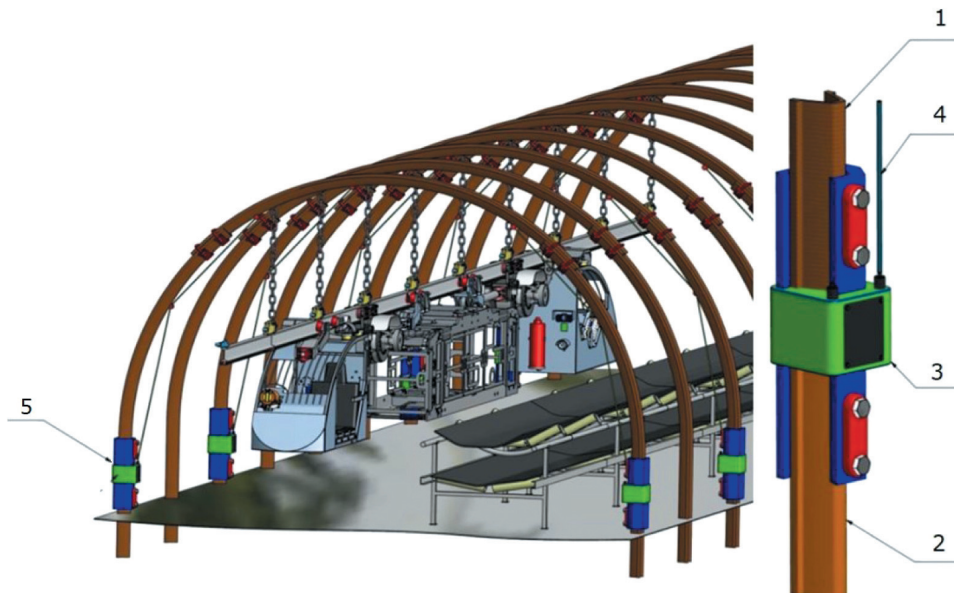


Fig. 2. Concept of installation measuring modules: 1 – upper part of wall-side segment, 2 – lower part of wall-side segment, 3 – data-processing module with sensors and data-transferring components, 4 – distance sensor cord, 5 – measuring module

2. VIBRATING WIRE STRAIN GAUGES

Problems with installing force transducers in underground conditions and the high cost of such transducers were the reasons for a market analysis to select another measuring method. Commonly used in the construction industry, vibrating wire strain gauges were selected [1]. These strain gauges are much cheaper (costing about 10% of the force transducer price) and they offer a simpler assembly method that can be applied in mine undergrounds on existing sup-

port frames (e.g., by sticking them to the assembly handles). Strain gauges of such a type can be easily adapted for the requirements of the ATEX Directive by placing them in special encapsulation and connecting them to the intrinsically safe measuring system. The linear characteristics of wire vibrations depending on deformations is an important advantage of such strain gauges. The design of such strain gauges provides the possibility of using them under difficult atmospheric conditions. The manufacturer informs us that they maintain their operational parameters

for up to 25 years in the construction industry [2]. However, the lifetimes of these strain gauges can be shortened due to the corrosive conditions in underground mines.

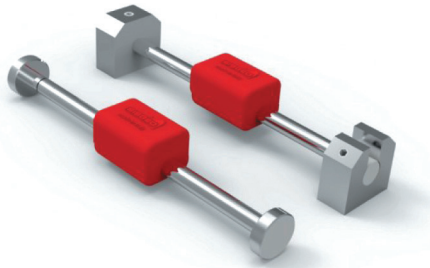


Fig. 3. Sample vibrating wire strain gauges [2]

The strain gauges have a steel wire stretched between two assembly points (Fig. 3). Changes in the distance between these points causes changes in the wire vibration's frequency, which is read by a periodically operating electromagnet (excitation – reading). The electromagnet is controlled by a dedicated reader, for example; in the discussed case, it is controlled by the intrinsically safe measuring system.

3. TESTS WITH USE OF WIRE STRAIN GAUGES

3.1. Stand tests

As part of the project, initial tests were carried out to investigate the applicability of a vibrating wire strain gauge for the strain measurements (loads) of an arch support. The strain gauge (mounted on a 30 cm section of the V29 profile) was loaded on a testing facility at KOMAG (Fig. 4). The strain gauge was mounted by welding the handles on the side of the profile. When choosing the mounting location, the available space and safety aspects of the strain gauge itself were considered, as the device would be exposed to damage in a mine.

During the test, the vibration frequency of the wire was recorded when the profile was loaded with a force of between 0 kN to 400 kN (the maximum force possible to exert). The test confirmed the linear characteristics of the vibrating wire strain gauge. Figure 5 presents a diagram of the proportional dependence of frequency versus the applied force.



Fig. 4. Testing facility at KOMAG

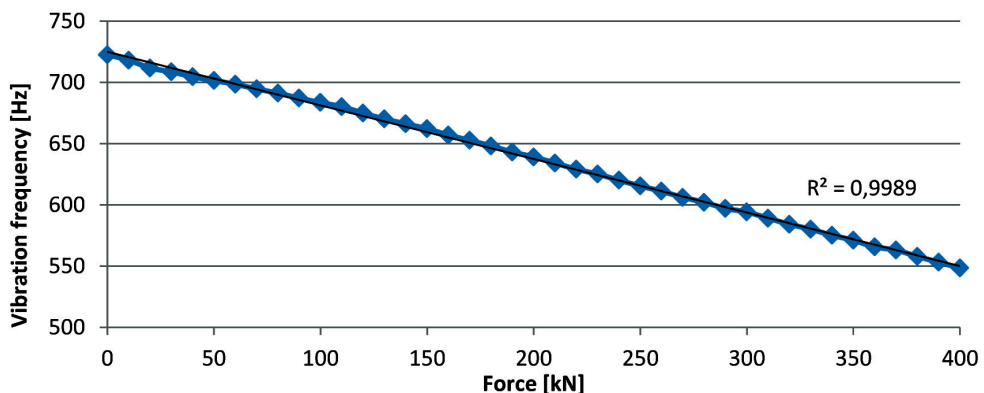


Fig. 5. Diagram of relationship between wire frequency and force

After transforming the results according to relationship (1), one can obtain the strain value given in the literature as a microstrain, which is a dimensionless quantity often expressed in $\mu\text{m}/\text{m}$ or $\mu\text{inch}/\text{inch}$ [2]:

$$\mu\varepsilon = (f^2 \cdot 10^{-3}) \cdot G \quad (1)$$

where:

f – vibration frequency of wire [Hz],

G – measuring constant, provided by manufacturer in wire strain gauge's certificate [$1/\text{Hz}^2$].

Stand tests of the ŁPP10/V29/4/A/I arch support frame (carried out according to the diagram shown in Figure 6 in the testing facility (Fig. 7) of the Central Mining Institute) was the next step for collecting data from the wire strain gauges [3].

The wire strain gauges and additional film strain gauges (for comparison) were mounted on both sides of the support frame on one side of the V profile in the lower part of the side wall arch (Fig. 7).

The arch support frame is loaded from the roof side by three hydraulic cylinders: F4, F5, and F6. The response from the side wall was mapped using six hydraulic cylinders according to the diagram shown in Figure 6. Additionally, the slides were recorded in the joints between the roof arch and the side wall arch during the measurement using two draw-wire displacement sensors. During the test, the lowered height of support frame ΔW was also recorded in an indirect way by measuring the extension of the actuator F5 loading the support frame in its axis of symmetry.

The time process of the forces is presented in Figures 8–10.

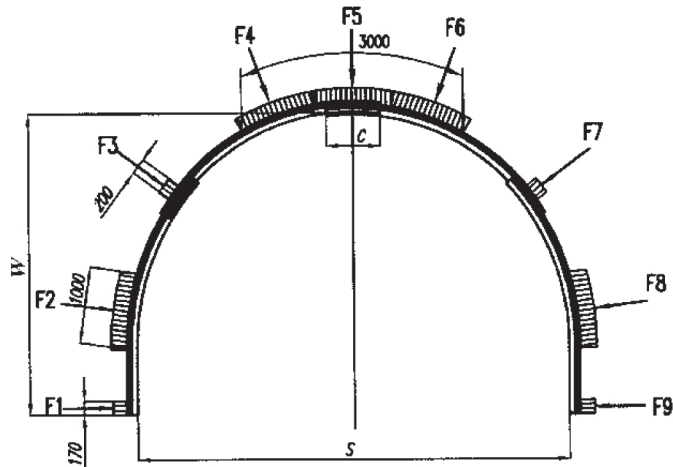


Fig. 6. Diagram of loading ŁPP10/V29/4/A/I arch support frame during stand tests:
F4, F5, F6 – active forces; F1, F2, F3, F7, F8, F9 – reaction forces (so-called passive resistance forces) [3]

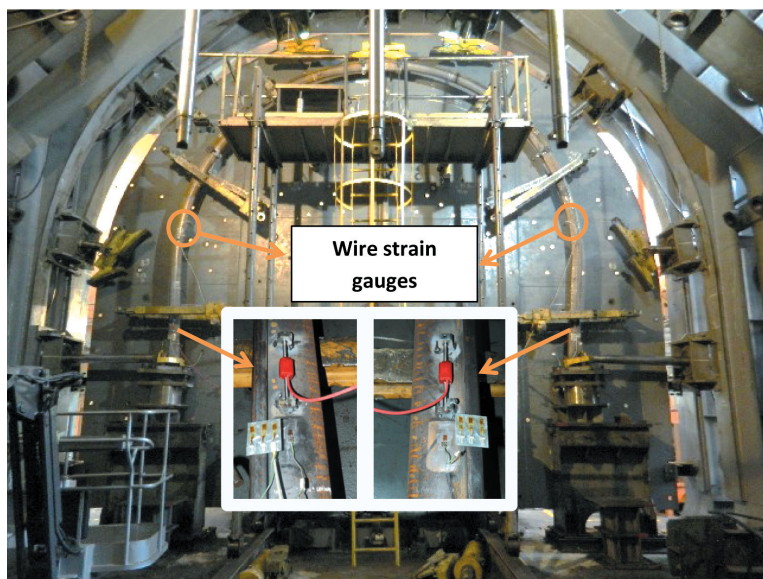


Fig. 7. View of testing facility

Figure 8 shows the time process of the applied force determined arithmetically by measuring the pressure in the F4, F5, and F6 cylinders in the hydraulic system after loading the tested object. The periodic increases in force and subsequent sudden drops were caused by sliding occurring on the joints of the roof support.

Figure 9 shows the time process of the deformation obtained from the film strain gauges. The re-

corded values are negative because the strain gauges were compressed. The right strain gauge worked properly, perfectly reflecting the dependence of the strain on the applied force. The increase in force caused an increase in the deformation, while the slide and the associated drop in force caused a sudden reduction in deformation. Halfway through the test, the left strain gauge indication was close to 0; then, the indicated values suggest roof support compression.

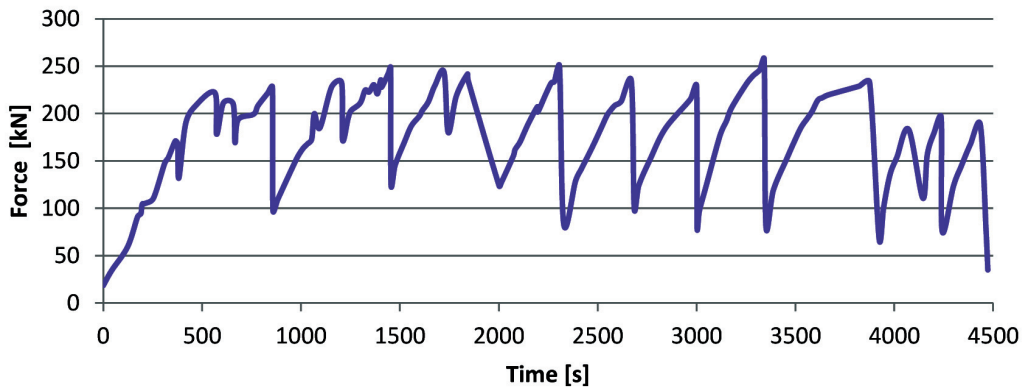


Fig. 8. Test procedure – force determined from pressure in hydraulic system

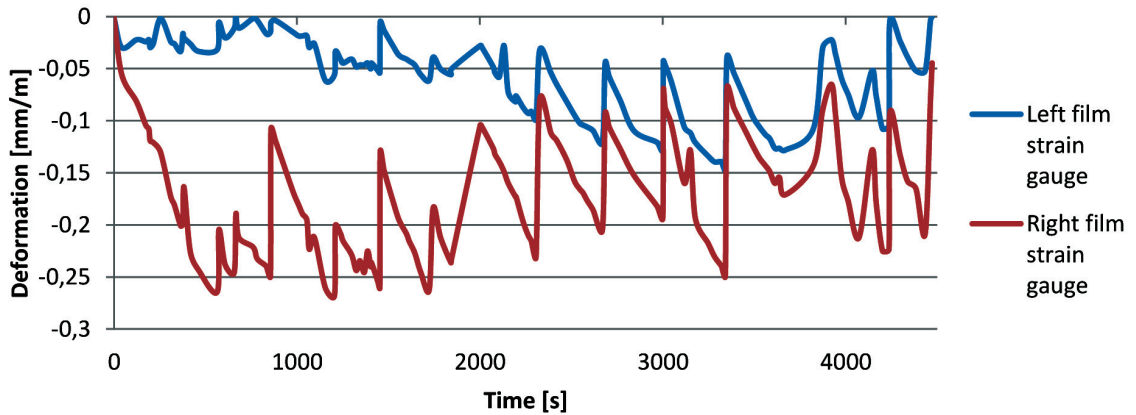


Fig. 9. Time process – deformations from film strain gauges

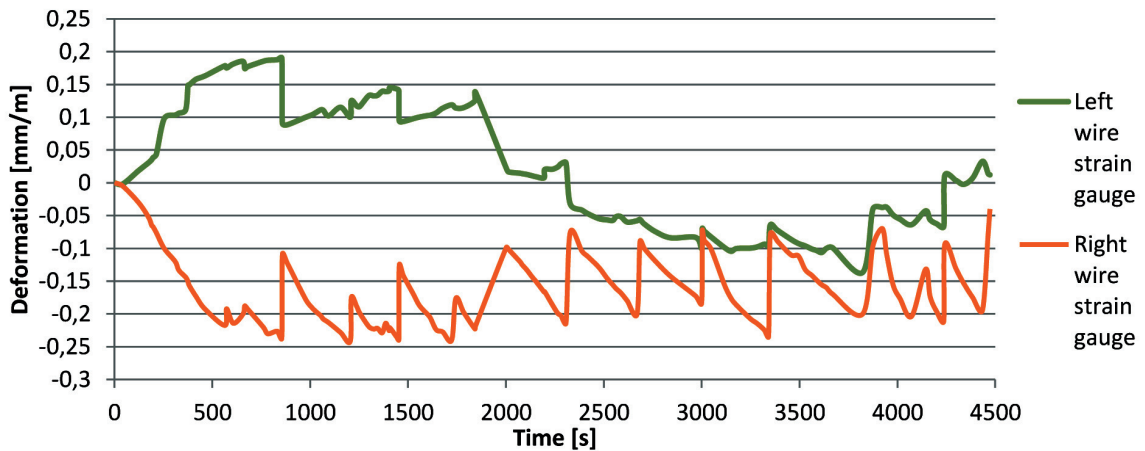


Fig. 10. Time process – deformation from wire strain gauges

Figure 10 shows the results obtained from the vibrating wire strain gauge. The reader dedicated to the purchased wire strain gauges was used to enable the direct reading of the deformation [mm/m]. As in the case of the strain gauges, the right wire strain gauge mapped the force indications (as well as the negative values related to wire contraction). In the case of the left strain gauge, the results suggested that the arch support was stretched at the point of the wire strain gauge installation.

The data from the wire strain gauges recorded during the tests are compared and presented in Figures 11 and 12.

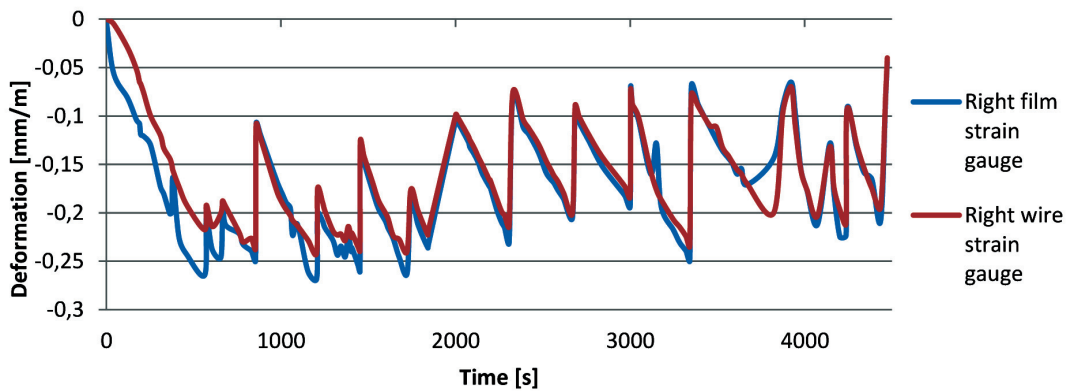


Fig. 11. List of results – right side

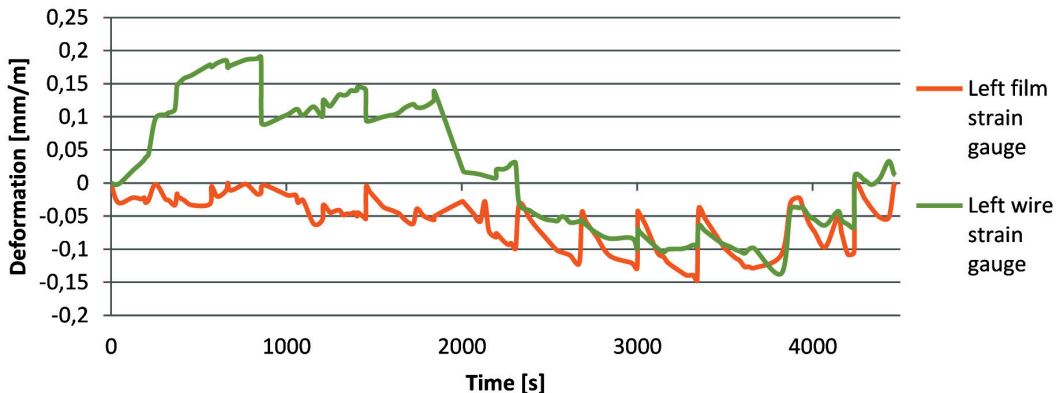


Fig. 12. List of results – left side

The conclusions that have been drawn from the conducted tests are based mainly on the fact that the support on which the tests were carried out was already loaded (as a part of other tests). In addition, the loading cylinders slightly deformed the right side of the roof support, and the component transferring the main load was twisted during the test (Fig. 13). This could have increased the pressure on the right side of the roof support.

Also, the straight sections of the wall arches were bent inwards, which could also have an impact on the uneven load distribution in the tested object.

Figure 11 shows that the recorded deformation and slide values are very similar on the joints of the support (both from the right wire strain and right film strain gauges).

From the comparison of the left side (Fig. 12), it appears that the measurements from both film strain gauges differed from the expected values. The film strain gauge operated within the region of a zero value, whereas the wire strain gauge showed a significant stretching of the string. This condition changed at one point, and both the film strain and wire strain gauges began to indicate values suggesting support compression.



Fig. 13. Visible rotation of component transferring main load

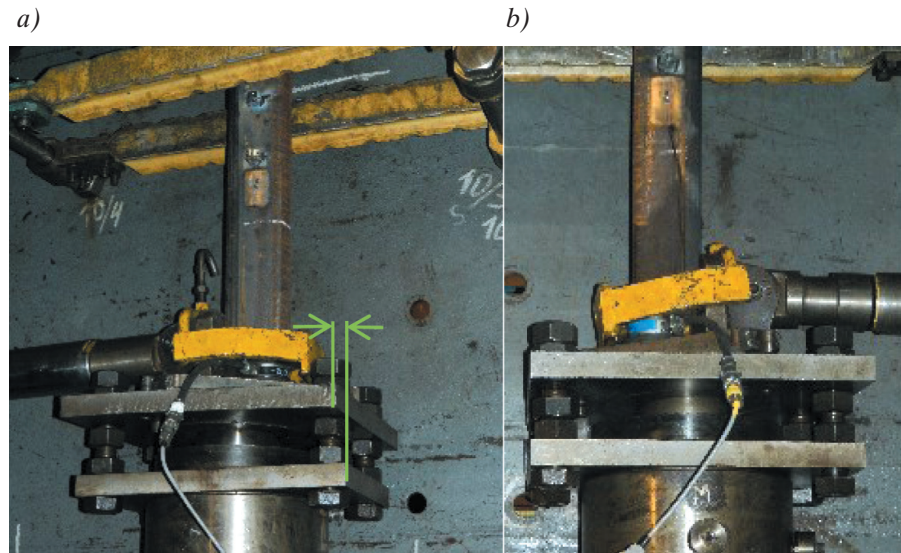


Fig. 14. View of plates under arch support: a) left side; b) right side

This also suggests a displacement of the steel plate located under the left side of the sidewall part of the frame, which was in line with the bottom plate before the test (Fig. 14a).

All of these factors could have caused a bending moment on the left side of the tested object (in the place where the sensors were installed). The readout of the wire strain gauge subjected to bending indicated the suggested stretching. The film strain gauge generated results close to zero, as it could compensate itself if it were bent in the measuring axis (a part of the strain gauge was stretched, and a part of it was compressed).

On one hand, the test results give us hope for the positive use of wire strain gauges to measure the deformation of a support and indicate the need to analyze the locations of the sensors' installation. As a result, further tests are planned in which the sensors will be installed on top of the bottom of the V-profile (on the side facing the roadway). The profile here has the thickest cross-section, and the bending impact on the test result will be smaller. Repeated tests should be carried out on a new roof support that will allow us to minimize the possibility of ambiguous results.

At this stage, it should be emphasized that the results obtained from the stand tests make a valuable contribution to the expert system, whose task will be to assess the operating conditions of the support in terms of increasing the speeds of suspended monorails. Thanks to the collected data, it will be possible to analyze the possibility of installing sensors with a vibrating wire on a roadway support that shows signs of deformation.

3.2. Numerical strength calculations

Numerical strength calculations were used to determine the impact of the boundary conditions as well as the position of the strain gauges on the results. The conditions of the testing facility were recreated in the computational model and developed in the software environment using the FEM method [4]. There is also a possibility for recreating a complete support arch and apply an impact load to it [5]. However, for the purpose of the current task, the computational model included a section of the roadway support's side wall arch of a size of LP10 and a profile of V29. The geometrical model was discretized and a finite element grid was created; this consisted of spatial elements of the HEX8 type with an average square side dimension equal to 3 mm (Fig. 16).

At that point, the boundary conditions were entered. The computational model was fixed to the bottom surface (marked in blue in Fig. 16). To eliminate the friction resistances, each nod laying on two parallel planes (upper and bottom) had the possibility of moving along these planes. Compressing force F was equal to 400 kN (Fig. 16). Besides, the nod on which the compressing force was exerted could only move along the OZ axis to eliminate model buckling.

Based on the strength calculations in the linear range, the results of the FEM numerical calculations were obtained (Fig. 17).

The calculation results show a high compliance with the stand test results. They present a linear increase of the displacements as well as the same reduced stresses and directional deformations in the entire volume of the computational model (the same value for all legend colors).

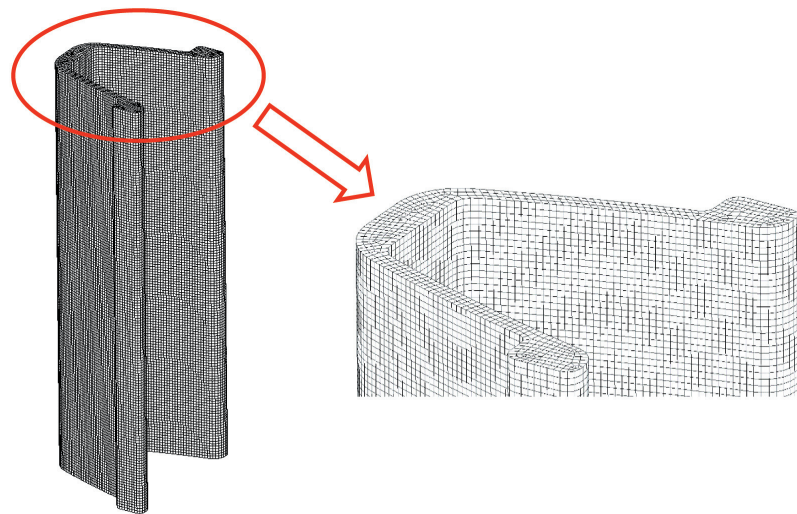


Fig. 15. Spatial grid of computational model of roadway support's side wall arch



Fig. 16. Boundary conditions in computational model

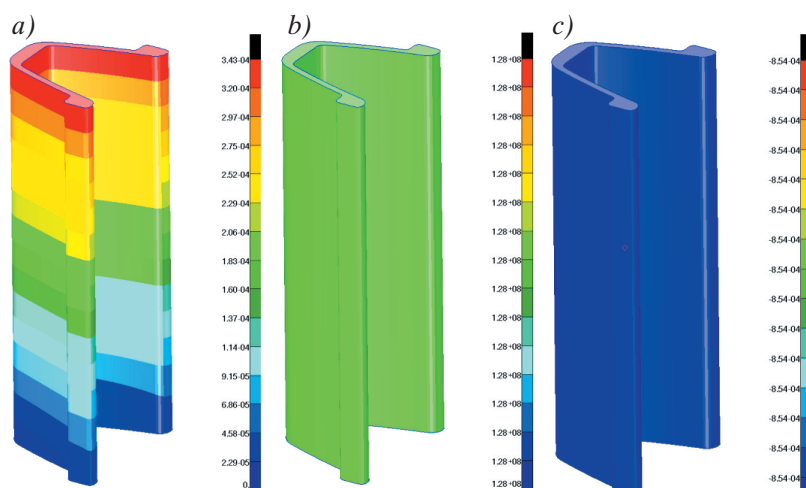


Fig. 17. Results of FEM calculations: a) map of displacements [m]; b) map of reduced stresses [Pa]; c) map of directional deformations

Linear deformations at any point of the object are defined as the quotient of the difference between the initial and end values of the given finite element and the end value (resulting from the acting load). The computational model was validated to fit it into the range of the material parameters (characteristics).

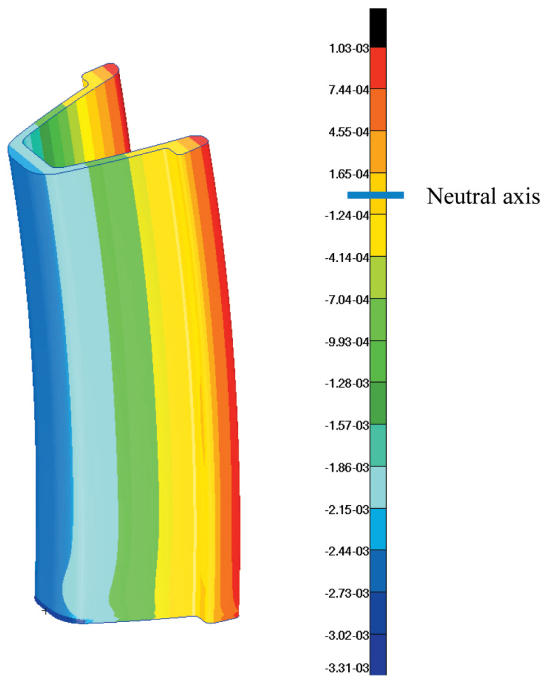


Fig. 18. Results of calculations for edge support of side wall arch section – map of directional deformations (neutral zone marked in light orange)

Then, a fulcrum of the computational model was introduced, which resulted in a significant difference in the directional deformations depending on the position of the strain gauge in the transverse cross-section of the arch support (Fig. 18). This is a result of torque, as the edge of the support does not cross the loading force axis.

4. MEASUREMENTS OF SUPPORT GEOMETRY

The support geometry was measured by draw-wire sensors. Draw-wire sensors measure the position of and monitor the movement of an object by the use of a measuring wire wound around a drum [6]. The wire end is fixed to the tested object, and the sensor is fixed to a stable base. Displacement of the tested object sets the measuring drum into motion. A multi-turn potentiometer is connected to the drum (Fig. 19).

The potentiometer (variable resistor) in the intrinsically safe circuits is treated as a passive element that does not need a certificate. Such a solution extends the possibility of using sensors from different manufacturers. The problem of protecting the sensors against environmental impact (temperature, humidity, dust, etc.) can be solved by placing them in an additional enclosure.

In Figure 20, the time processes of the slides recorded on the roof support joints by the draw-wire sensors are presented. The results have positive values due to the method of calibrating the measuring instruments during the test. The sensors were placed on both sides of the arch support joints in such a way that the wire is run from the sensor to the fixation point behind the joint. The wire made a chord of the arch section behind the joint, so it was not a direct measurement of the joint slide but merely an approximate value (to enable us to assess the result).

In Figure 21, the slides (ΔW) in the joints of the support frame as the difference between the thick lines drawn on the tested arch components are presented. The recorded readings of the left and right sensors can be transformed into the slides.

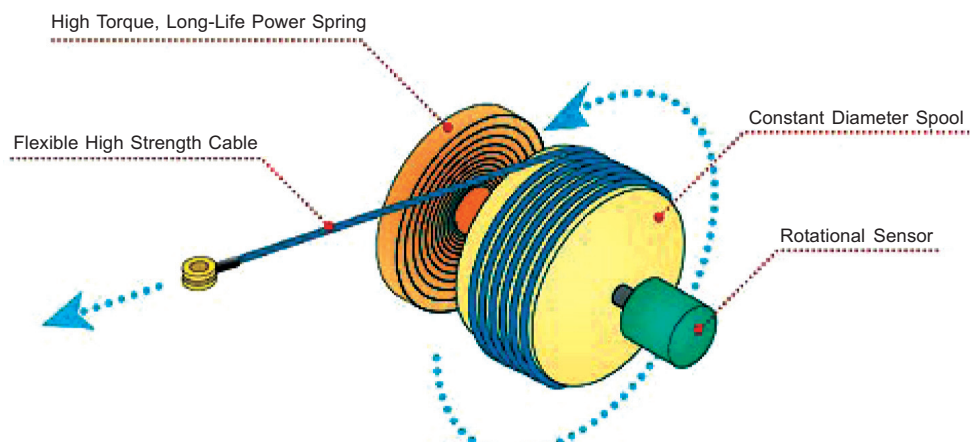


Fig. 19. Draw-wire sensor [6]

The upper draw-wire sensor recorded the cylinder extension, which can be transformed into a total reduction in the support height as a result of the slides in the joints including elastic deformation and changes in the position of the support's frame. Measurements of the slide between the arch components will enable us to determine the current geometry of the support's

frame (without the deformation resulting from the elastic and plastic deformations).

Under actual conditions, changing the support height will only be measured by draw-wire sensors placed directly on the arch support. The number of installed sensors will depend on the number of support joints.

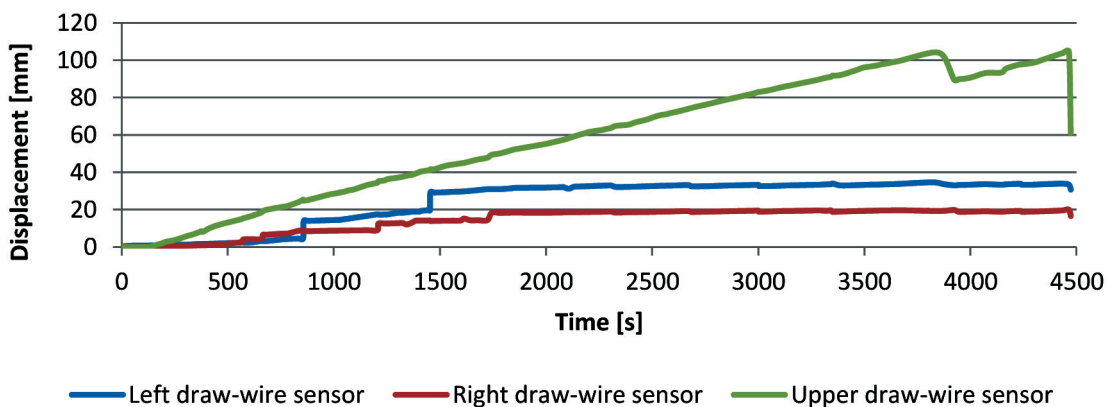


Fig. 20. Results of displacement measurements with use of draw-wire sensors

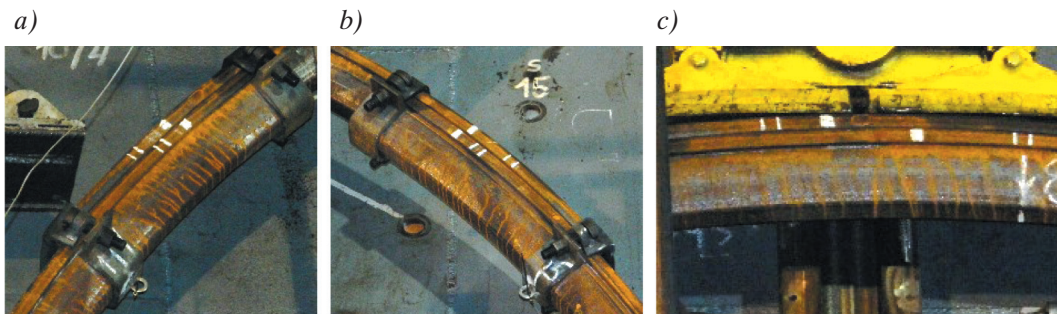


Fig. 21. Slide on support's frame joints: a) left side; b) right side; c) center

5. CONCLUSIONS

Being used to monitor building structures more and more often, strain gauges with vibrating wires also work well when measuring the deformation of an arch support's frame. Their high sensitivity ensures a stable reading even at the slightest load to the support's frame. The strain results obtained from wire strain gauges are comparable to those obtained from film strain gauges. Due to the ambiguous test results recorded on one side of the arch support's frame, additional tests should be carried out with a different sensors arrangement. It should be noted that the measurement is burdened with errors resulting from the operating conditions of the arch support and co-operation with the stand (e.g., warping, movement of the supports, uneven load, or deformation of the supports). In the case of underground tests, more diffi-

culties should be expected due to the difficult working conditions.

Measuring the slide between roof support components using wire strain gauges in a targeted measurement system will allow us to assess any changes in the support geometry.

The strength calculations showed a great compliance with the results of the stand tests. Their aim will be to indicate specific locations for placing a wire strain gauge or film strain gauge, especially in the case of non-planar support of an object.

Acknowledgements

The article was developed with the INESI (Increase efficiency and safety improvement in underground mining transportation routes) project (Contract No. 754169) financed from the Coal and Steel

Research Fund. The numerical calculation were realized on a computer belonging to the Academic Computer Center in Gdańsk – TASK.

Bibliography

- [1] Bednarski Ł., Sieńko R.: *Pomiary odkształceń konstrukcji przetwornikami strunowymi*, “Inżynieria i Budownictwo” 2013, 11: 615–619.
- [2] www.sisgeo.com/products/strain-gauges-and-thermometers/item/corda-vibrante.html
- [3] Pytlik A.: *Stanowisko i metodyka badań obudowy podporowej-kotwiowej w skali naturalnej*, “Przegląd Górnictwa” 2017, 73, 8: 18–23.
- [4] Zienkiewicz O.C., Taylor R.L., Zhu J.Z.: *The Finite Element Method. Vol 1: Its Basis & Fundamentals. Vol 2: For Solid and structural mechanics*, Sixth edition. Elsevier Butterworth – Heinemann, Oxford 2005.
- [5] Tokarczyk J., Winkler T.: *Numerical simulation of dynamic impact of loads, transported by suspended monorails, on yielding arch supports*, “Coal International” 2013, 5: 47–51.

- [6] www.dacpol.eu/pl/zasada-dzialania-linkowego-przetwornika-odleglosci-przeglad-dostepnych-typow/product/zasada-dzialania-linkowego-przetwornika-odleglosci-przeglad-dostepnych-typow_CELESCO.

*MARIUSZ WOSZCZYŃSKI, Ph.D., Eng.
JAROSŁAW TOKARCZYK, Ph.D., Eng.
KRZYSZTOF MAZUREK, Ph.D., Eng.
KOMAG Institute of Mining Technology
ul. Pszczyńska 3, 44-101 Gliwice, Poland
{mwoszczynski, jtokarczyk, kmazurek}@komag.eu*

*ANDRZEJ PYTLIK, Ph.D., Eng.
Central Mining Institute
pl. Gwarków 1, 40-166 Katowice, Poland
apytlik@gig.eu*